

Petrographic and mineralogical study of the sediment-hosted Cu-Co ore deposit at Kambove West in the central part of the Katanga Copperbelt (DRC)

Sander VAN LANGENDONCK¹, Philippe MUCHEZ¹, Stijn DEWAELE², Alphonse KAPUTO KALUBI³ & Jacques CAILTEUX⁴

¹ *Geodynamics and Geofluids Research Group, Department of Earth and Environmental Sciences, KU Leuven, Celestijnenlaan 200E, 3001 Heverlee, Belgium*

² *Department of Geology and Mineralogy, Royal Museum for Central Africa, Tervuren, Belgium.*

³ *Département Géologique, Gécamines, Likasi, D.R. Congo.*

⁴ *Département Recherche et Développement, E.G.M.F., Groupe Forrest International, Lubumbashi, D.R. Congo.*

ABSTRACT Kambove West is a sediment-hosted Cu-Co deposit in the Neoproterozoic Mines Subgroup, which is mainly composed of dolomitic shales and dolostones. Key factors and processes responsible for high-grade mineralization were identified by studying multiple cores. The stratigraphic position of the mineralized zones adjacent to the Roches Siliceuses Cellulaires and brecciated zones are the most important factor controlling the formation of a high-grade mineralization as they most likely acted as conduits for the mineralizing fluids. The presence of organic matter, stromatolite fragments and anhydrite pseudomorphs promoted mineralization. The organic matter caused a reducing environment required for the precipitation of the sulfides. Sulfate-reducing microorganisms, which were main components of Precambrian stromatolite communities, could also have caused the necessary reduction reactions. In addition to sulfate from the pores of the sediment, anhydrite formed a sulfate source.

A paragenesis with six stages was established based on microscopic observations and cold cathodoluminescence petrography. Two major hypogene mineralization phases, which consist of pyrite, chalcopyrite, bornite, chalcocite and carrollite, formed during diagenesis and low-grade metamorphism, and were succeeded by supergene remobilization, of which chalcocite forms the dominant Cu-phase in the cementation zone. The distinction between hypo- and supergene chalcocite is based on the identification of multiple microtextures, chalcocite polymorphism, and the association with iron and other (hydro)oxides or late generations of dolomite. However, none of the features are conclusive. The combination of them is highly suggestive for a supergene remobilization.

KEYWORDS: Neoproterozoic mineralization, stratiform Cu-Co ore deposits, Central African Copperbelt, Kambove West, ore distribution and grade, supergene enrichment, chalcocite

1. Introduction

The Central African Copperbelt (CACB) consists of Neoproterozoic rocks that host multiple types of deposits, of which the sediment-hosted stratiform Cu-Co type forms the most important one. The metal potential comprises 200 Mt of copper and >8 Mt of cobalt (Misra, 2000; Cailteux et al., 2005b). The Neoproterozoic (meta-)sedimentary rocks hosting the mineralization, form part of the Katanga Supergroup. This supergroup is present in the south of the Democratic Republic of Congo (Katanga Copperbelt) and the northwestern part of Zambia (Zambian Copperbelt).

Numerous models have been suggested for the Cu-Co mineralization in the Central African Copperbelt (Sweeney et al., 1991; Sweeney and Binda, 1994; Cailteux et al., 2005b; Selley

et al., 2005; Dewaele et al., 2006; El Desouky et al., 2008, 2010). Nowadays most authors agree about a multiphase origin for the sulfides, in both Zambia (e.g. Selley et al., 2005; Hitzman et al., 2005; Brems et al., 2009; Muchez et al., 2010) and the DRC (e.g. Cailteux et al., 2005b; Dewaele et al., 2006; Muchez et al., 2008; El Desouky et al., 2009, 2010; Haest & Muchez, 2011).

During the last decade, many Cu-Co deposits in the DRC have been again the subject of detailed studies: Kamoto (Dewaele et al., 2006; Muchez et al., 2008; El Desouky et al. 2009, 2010), Luiswishi (El Desouky et al. 2009, 2010), Kamao (Broughton & Rogers, 2010) and Tenke-Fungurume (Fay & Barton, 2012). This resulted in the reconstruction of detailed paragenetic sequences of mineral precipitation. The geological setting, lithostratigraphy, depositional environment of the sediments and mineralogy of the Kambove West deposit have been extensively studied in

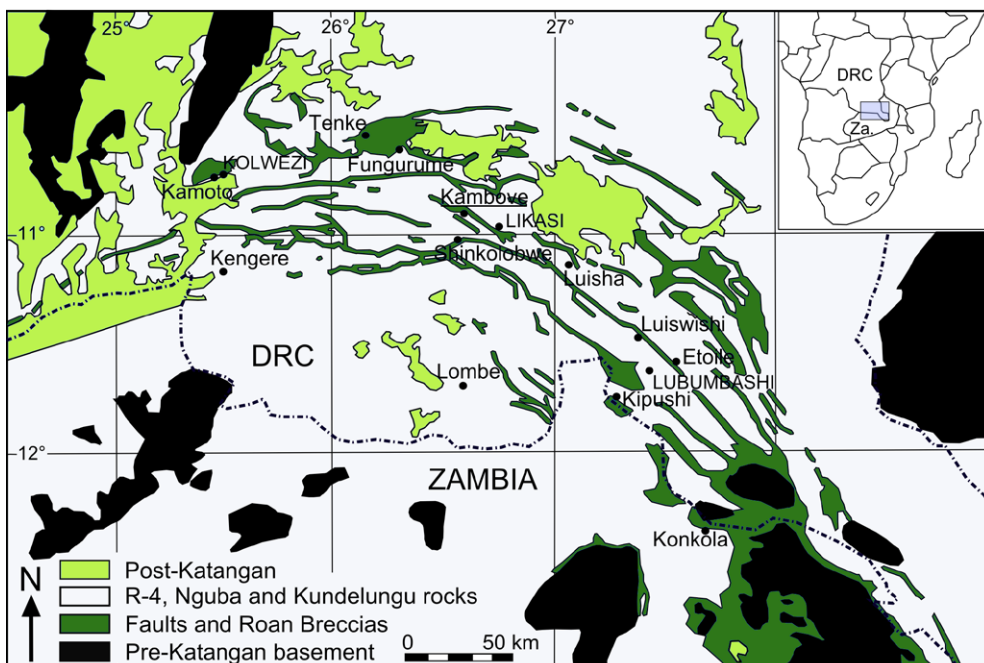


Figure 1. Geologic map of the Central African Copperbelt with the location of the Kambove deposit. Modified after François (1974), Cailteux (1994), and Cailteux et al. (2005b).

the past (Cahen et al., 1971; Cailteux, 1977, 1979, 1983, 1986, 1997; Cailteux et al., 2005a, b). The present study focuses on the paragenetic sequence of mineral precipitation and its relative timing, and on the relation of the ore grade with the different mineralizing processes at Kambove West. The distinction between hypogene and supergene processes is discussed. These processes are further compared with the metallogenetic processes proposed for the Katanga Copperbelt (cf. Dewaele et al., 2006; Muchez et al., 2008; El Desouky et al., 2010; Fay & Barton, 2012).

The Kambove region is located 25km northeast of Likasi (Fig. 1). The Kambove West deposit consists of a large north-verging syncline. The southern flank stands nearly vertically, while the northern flank lies almost sub-horizontal at a depth of 400-500m. As the southern flank crops out, it was the first to be exploited. Firstly, an open pit mine was in operation from 1959 to 1965 (François, 2006). From 1963 onwards, exploitation continued in the Kambove West underground mine (International Bank for Reconstruction and Development, 1974). Total production at Kambove West until January 1973 was 10.92 Mt ore at 5.68%. In 1978, the mineralization in the northern flank was discovered and the exploitation of this flank started in 1988. The mine, however, collapsed the same year and exploitation stopped (François, 2006). Before its closure, the Kambove underground mine had an annual production of 1.5 million tons of ore (Prasad, 1989). However, due to rising Cu and Co prices there is a renewed interest in opening the underground mine of this deposit.

2. Geological setting

During the early Neoproterozoic, the Rodinia supercontinent underwent continental thinning and extension. Sedimentation of the Katanga Supergroup started in an intracontinental rift setting significantly after 880Ma (e.g. Kampunzu et al., 2000; Armstrong et al., 2005; Johnson et al., 2007). The sequence starts with the RAT Subgroup (Fig. 2a), a massive and irregularly stratified detrital subgroup, which is often remarkably hematite-rich due to the primary oxidizing conditions (Cailteux et al., 2005a). Afterwards, evaporitic carbonate-rich sedimentary rocks of the Mines Subgroup were deposited in shallow intratidal to supratidal environments and hypersaline lagoons (Cailteux et al., 2005b). In these dolomitic shales and siltstones, relicts of stromatolites and algal reefs can be found. The Dipeta Subgroup is composed of argillaceous and siliciclastic beds at the base and carbonate beds at the top. The Mwashya Subgroup consists of carbonaceous and dolomitic shales and dolomites (Cailteux, 1994). Continued rifting resulted in the Roan sediments being conformably overlain by the Nguba en Kundelungu Groups. During the assembly of the Gondwana Supercontinent (~550Ma), the Khomas ocean was closed due to a transition in stress regime from extensional to compressional, which led to the collision between the Congo and

the Kalahari Cratons and the formation of the Lufilian fold-and-thrust belt, also called the Lufilian Arc (Kampunzu et al., 2000). This tectonic structure is north-verging, east-west oriented and ~700km long and more than 150km wide (Cailteux et al., 2005b).

There are multiple models for the thrust tectonics in the Lufilian belt. The most popular model involves an external fold-and-thrust belt formed by thin-skinned tectonics (Cosi et al., 1992; Kampunzu & Cailteux, 1999, and references therein). Basement-cover successions became duplicated by complex thrust repetition. Associated with the thrust sheets, large megabreccias are often found. These large blocks can reach sizes up to 10 kilometers and consist of rocks belonging to the RAT, Mines and Dipeta Subgroups (Cailteux & Kampunzu, 1994; Jackson et al., 2003). Porada & Berhorst (2000) stated that these major displacements were facilitated by mudflat deposits acting as thrust planes. This also explains the thrusting along the detachment planes in the lower part of the Roan Group. The evaporitic minerals from the mudflat deposits acted probably as lubricant during deformation (Porada & Berhorst, 2000). Also other authors indicated that the evaporites played a major role in the kinematics of the Lufilian Orogeny (e.g. François, 1987; de Magnee & François, 1988; Cailteux & Kampunzu, 1994; Kampunzu & Cailteux, 1999; Porada & Berhorst, 2000; Jackson et al. 2003, and references therein).

The occurrence of two or three orebodies in the Mines Subgroup is strongly controlled by the lithostratigraphy. The First or Lower Orebody occurs in the gray RAT (Roches Argillo Talqueuses), DStrat (Dolomies Stratifiées) and RSF (Roches Siliceuses Feuilletées) members of the Kamoto Formation. The Second or Upper Orebody is hosted by the SDB (Shales Dolomitiques de Base) or SD-1a (Shales Dolomitiques), the lowest members of the Dolomitic Shale Formation. Locally, also a Third Orebody, usually composed of multiple smaller ore lenses, is present in the CMN-11 and CMN-12 (Calcaire à Minerai Noir) at the base of the Kambove Formation. Sub- to slightly economic deposits are also found in organic-rich, black, carbonaceous, metapelitic horizons of SD-2d and SD-3b. The close relationship between the presence of metals and organic matter indicates deposition in a strongly reducing environment (Cailteux et al., 2005b).

A first mineralization phase contains, in addition to authigenic quartz, sulfides that are either disseminated or occur in nodules, lenses and bands (El Desouky et al., 2009, 2010, type I nodules). Prior to these sulfides, a dolomitization event took place in lenses, bands and nodules (Mucchez et al., 2008). Mineralization took place by an evaporated seawater (11.3-20.9 wt% NaCl equiv). The infiltrated seawater was heated (>115-220°C) in the deeper subsurface and became enriched in radiogenic strontium and (likely) Cu-Co metals during migration through the basement

(a) KAROO and KALAHARI				(b)				
Group	Subgroup	Formation	Member	Ore	Com. thick. (m)	Kam. thick. (m)		
Katanga Supergroup	Kundelungu (Ku)		Upper Kambove (R-2.3.2) (Formerly Upper Calcaire à Minerai Noir or Upper C.M.N.)		40-100	>2.6		
							Nguba (Ng)	
	Roan (R)	Dipeta (R-3)	S.D.-3b	Upper Orebody	30-125	>20		
			S.D.-3a					
			S.D.-2d					
			S.D.-2c					
			S.D.-2b					
			S.D.-2a					
	Mines (R-2)	Dolomitic Shale (R-2.2)	Shales Dolomitiques de Base (S.D.B.; S.D.-1a)		Upper Orebody	5-15	8-17	
			Kamoto (R-2.1)	Roches Siliceuses Cellulaires (R.S.C.)	Lower Orebody	6-12.5	18.5	
				Roches Siliceuses Feuilletées (R.S.F.)				
	R.A.T. (R-1)	Dolomites Stratifiées (D.Strat.)						
			Roches Argilo Talqueuses grises (gray R.A.T.)					0.5-5
	Base of the R.A.T. sequence - unknown							
	Basal conglomerate							
KIBARAN and PRE-KIBARAN								
± 880 Ma								
± 2050 Ma								

Figure 2. A: Lithostratigraphic subdivision of the Katanga Supergroup in the DRC (Data from Cailteux et al., 2005b; Batumike et al., 2007). B: Detailed lithostratigraphy of the Mines Subgroup with the common thickness range (Com. Thick) of these units in the Katanga Copperbelt. The location of the three typical stratiform Cu-Co orebodies is indicated as well (Data from Cailteux et al., 2005b). After El Desouky et al. (2010).

rock (El Desouky et al., 2009). The evaporite nodules and layers, together with organic matter, allowed bacterial sulfate reduction (BSR) to take place during diagenesis. The most common ore minerals are chalcopyrite, bornite and minor chalcocite and pyrite (Cailteux et al., 2005b; Selley et al., 2005). Sulfide precipitation also occurred in nodules of type II, veins, spots and as cements in tectonic breccias (Cailteux et al., 2005b; El Desouky et al., 2010). The type II nodules are coarser grained than the type I nodules and sulfides. Remobilization of the minerals formed during the first phase, is likely (El Desouky et al., 2009, 2010). The remobilization probably occurred during the Lufilian Orogeny (Cailteux et al., 2005b, and references therein). Fluid inclusion data confirm that the mineralizing fluid was indeed considerably hotter (270-385°C) and more saline (35.0-45.5 wt% NaCl equiv) than the fluid circulating during the first phase (El Desouky et al., 2009). The metal-bearing fluid migrated relatively easily through the Roan host rocks aided by brecciated zones, i.e. along faults and between the megabreccia blocks (El Desouky et al., 2010). No evidence has yet been found for fluid interaction with the basement rocks during this second mineralization. The sulfur in the second phase originated from (1) H₂S generated by TSR, (2) the sulfides of the first phase and (3) the earlier diagenetic pyrites (Cailteux et al., 2005b; El Desouky et al., 2010).

In both the DRC and Zambia, significant supergene enrichment occurred during weathering. The general model is that copper and cobalt were dissolved in the leached zone by meteoric water, which percolated downwards. Subsequently, the remobilized metals accumulated in the supergene blanket. Above the redox barrier, metals precipitated as oxides like heterogenite and carbonates, such as malachite. Under the redox barrier, mineralization occurs as sulfides, which is mainly chalcocite in the CACB. The redox barrier is usually the water table, but can also be a rock buffer (Webb & Rowston, 1995; Robb, 2005). Apart from the formation of new minerals, the secondary enrichment provides a major increase in the Cu and Co grade. The presence of voids is one of the main factors in the supergene enrichment, causing a high permeability and porosity and providing space for the secondary ore minerals to precipitate (De Putter et al., 2010). Decree et al. (2010) and De Putter et al. (2010) indicated that formation and possibly the enlargement of existing voids resulted from recent uplift, erosion, weathering, dissolution and karstification. Decree et al. (2010) stated that the presence of mobile Cu²⁺(aq) is due to the oxidation of Cu-sulfides during exposure to oxidizing agents. The distribution of the supergene minerals formed by the aqueous copper is linked to fluctuations of the water table. Those fluctuations could either be tectonically, climatically or seasonally controlled. As cobalt is less mobile, it remains near the surface to form heterogenite cobalt caps. The more mobile metals remain in solution and are able to percolate deeper

(Decree et al., 2010). Finally, bacteria are known to have played a role in leaching and deposition of Cu in certain deposits. This could also have been the case in Katanga but needs further investigation (De Putter et al., 2010).

3. Macroscopic description

Since the Kambove West underground mine is at least partly collapsed and has been abandoned for many years, research focuses on the numerous boreholes that were made in the early 70's. The cores from Kambove West, as well as from other locations in the Copperbelt, are stored in the Département Géologique de la Gécamines in Likasi. The available profiles from Kambove West are spaced by 30m and have a N20W - S20E orientation, parallel to the central 0 section (Fig. 3).

From the more than 100 boreholes that are available from the Kambove West deposit, three were selected (KW201bis, KW205 and KW213). Next to the required availability and completeness, also the orientation to bedding and depth, and thus the number of crossed stratigraphic members, were used as criteria during the selection of suitable boreholes. The three cores are projected on the 0 section (Fig. 3). 45 samples were taken from those three cores. These samples represent the great variety of different rock types and are more or less evenly distributed. Although there was a certain focus on copper- and cobalt-rich samples, also barren and poorly mineralized samples were taken. The thicknesses of the different members vary quite strongly. The SD-2a member is missing in core KW201bis.

The Gray RAT, DStrat and RSF form the First (or Lower) Orebody. The host rock is a light to dark gray dolomitic, clay-rich siltstone. While the Gray RAT is lighter in color and more homogeneous, rocks from DStrat and RSF are darker and layered. Some evidence of small-scale slumping and faulting structures and differential compaction around nodules is present. The nodules, bands and layers are made up of dolomite and quartz and often contain spots of chalcocite. All three members are crosscut by bedding normal veins of coarse white to pink, dolomite. Also fine, irregular veins of brownish dolomite and beige to white dolomite frequently crosscut all former structures. The mineralization consists of disseminated chalcocite in the host rock, chalcocite concentrated along the bedding and in bedding-parallel layers. Coarse chalcocite crystals are found at the margin of the coarse crystalline veins (Plate 1A). Pink cobaltoan dolomite replaces dolomite, especially a white, coarse crystalline variant. Rocks from the RSF are the most mineralized of the three members, while the Gray RAT is the least. Locally, the Gray RAT is strongly brecciated, and forms one of the main components of the BH (Brèche Hétérogène or heterogeneous breccia). The breccia consists of mm- to cm-scale fragments of grayish dolostone. The matrix consists of dolomite and quartz, but contains also a significant

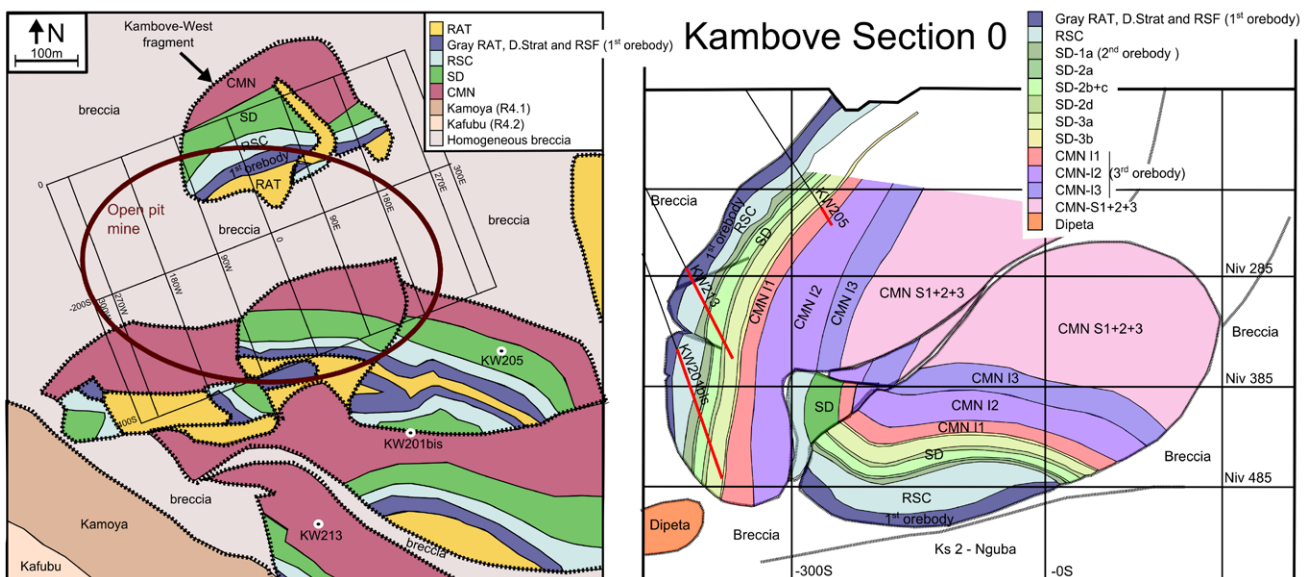


Figure 3. Geologic map of Kambove-West with the mine coordinate system and associated profiles, the old mine and the investigated boreholes. The red lines on the boreholes represent the part studied in this paper. Based on Cailteux (1983) and the Gécamines Département Cartographique.

amount of chalcocite and iron oxides/hydroxides, i.e. goethite and hematite. Some fragments have a red hue, especially at the margins due to oxidation.

The RSC-member is heavily altered, silicified and porous. Little is left of the original rock, which was a clay-rich dolostone with stromatolites (Cailteux et al., 2005b). Large spots to thick veins of very coarse white dolomite are abundant. Locally brecciation can be observed, often in combination with dissolution and other alteration features. In addition to dissolution, the alteration is characterized by the red coloring and thus oxidation of the rocks. Although the RSC is mostly barren (Cailteux et al., 2005b), chalcocite is abundant in this member at Kambove West. It occurs mainly as spots and in veins in the altered zones. In some

places spots of carrollite are left, often partly replaced by chalcocite. Frequently, next to big spots of chalcocite goethite and hematite are observed. A late phase of pink cobaltoan dolomite or spherocobaltite is very distinct. It can be replacive or infill pores and vugs.

The first member of the Dolomitic Shale Formation is the SDB or SD-1a and forms the Second Orebody. It consists of finely laminated gray dolomitic shales with many nodules, lenses and bands of dolomite, quartz and ore minerals (Plate IB, C). Strong differential compaction around these nodules took place, with a wavy appearance as consequence. Locally, levels of typical black shales can be observed that show an enrichment in organic material. Minor layer parallel veining and some irregular veins of

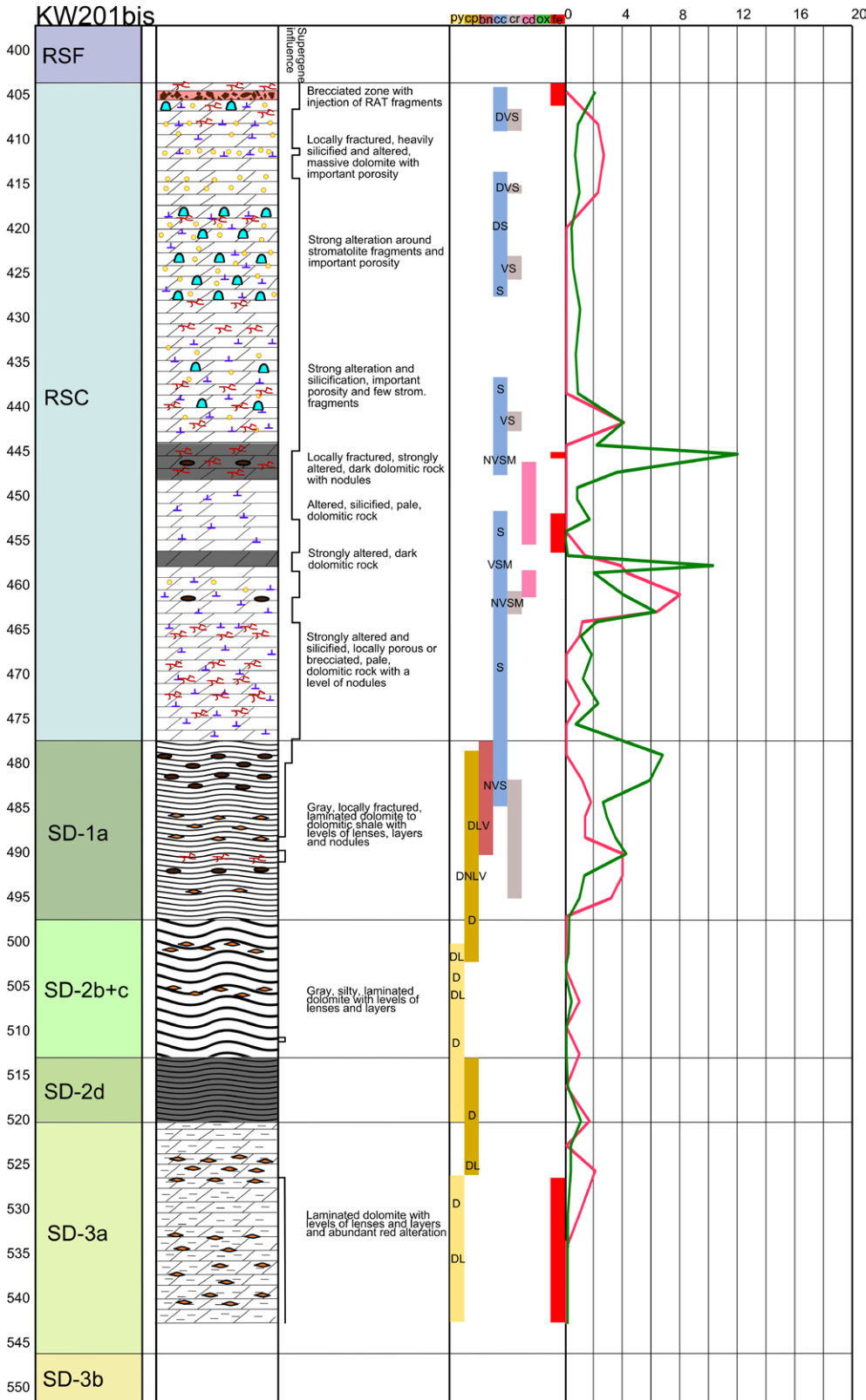


Figure 4. Stratigraphy, lithostratigraphic column, extent of the alteration, occurrence of the different ore minerals and grades of core KW201bis.

dolomite and quartz are present. Mineralization occurs disseminated, as spots, nodules and in bands. Ore minerals include chalcocite, bornite and chalcocite. The latter is especially abundant in the black shales as impregnation, and in altered zones as large irregular spots and veins. No relicts of carrollite nor cobaltoan dolomite were observed. The mineralogy consists of a rather simple association, with relatively few indications for alteration and reworking, except for the impregnated zones.

The younger SD-2a up to SD-3a members are also made up of finely laminated dolomitic shales. The shales are usually lighter in color, though dark organic-rich shales can occur. Nodules, lenses and bands as in SD-1a are lacking from these stratigraphic levels onwards. Layer parallel veins are abundant, but also layer normal and irregular veins are present. Differential compaction took place around several veins. At other places, an irregular silicification front, and bleached or brecciated zones can be observed. Pyrite, chalcocite and bornite make up the largest part of the mineralization. Locally, a massive replacement by or strong enrichment in chalcocite is observed. When chalcocite is abundant, the adjacent host rocks are mostly altered as indicated by the reddish color due to the presence of hematite or goethite. Sometimes, even malachite is observed. Minor quantities of cobaltoan dolomite are recognized.

The CMN (CMN-I1 – CMN-I2) consists of a gray layered to mainly massive dolomite, which is often quite dark due to the presence of organic material. Relicts of algal mats can be observed, analogous to the RSC. Dolomite-quartz bedding-parallel veins, bedding-normal and irregular veins are present. In many places fracturing and brecciation took place. Alteration is often very abundant in the form of light gray to beige fine crystalline dolomite. Also, the red color of iron oxides/hydroxides is clearly notable. Quite a lot of pink cobaltoan dolomite or spherocobaltite can be observed, especially near big spots of carrollite. Chalcocite is present in small to large spots, veins and replacing carrollite. In addition to a significant quantities of hematite and goethite, native copper, malachite, pseudomalachite, heterogenite and manganese oxides are present.

4. Ore grades

The ore grades from historical assays of the Gécamines (unpublished data) have been used to investigate the grade variation along the investigated boreholes.

In core KW201bis (Fig. 4), the RSC is in general intensely altered (oxidized and dissolved). Chalcocite occurs often as irregular spots. The minor increase in the copper content at 405m (2%) coincides with a brecciated zone at the top of the RSC. A little lower, a broad cobalt peak is found (405-420m). Carrollite occurs disseminated in the matrix and in veins. A close association of stromatolite fragments and carrollite was observed several times throughout the RSC (Plate 1D). Next to the fracturing and dissolution accompanied with silicification, also the local occurrence of iron oxides/hydroxides in this zone is quite distinct (Plate 1E, F). Between 444 and 448m, a major copper enrichment is observed in a dark organic-rich dolomitic rock (up to 12%). A significant amount of nodules and intense fracturing is also present at this depth. The copper occurs as chalcocite in nodules and veins, in spots and as a massive replacement. About 10m lower, a similar zone is present, except for the lack of nodules. Around 460m, a copper enrichment (10%) is found associated with nodules. Minor peaks (2%) are found in the lower part of the RSC, where the rock is intensely fractured and silicified. The major cobalt enrichment at 460m (0.8%) is linked to carrollite in nodules and veins and a replacement by cobaltoan dolomite.

In the SD Formation, the extension of the occurrence of altered rocks and the supergene influence decreases quickly, as does the copper grade, which is also reflected in the mineralogy. At the base of the SD-1a member, chalcocite, bornite and chalcocopyrite are found in nodules, veins and spots. From 485m onwards, bornite and chalcocite occur disseminated and in lenses, layers and veins. Below, only chalcocopyrite is found disseminated, in lenses, layers nodules and veins. When the copper grade is below 1%, chalcocopyrite occurs only disseminated. In the SD-2b+c and -d members, virtually no copper is left and only pyrite is present, disseminated and occasionally also in veins and layers. At

the base of the SD-3a member, some chalcocopyrite is found disseminated and in lenses and layers. From about 525m onwards, pyrite occurs mainly disseminated and locally in lenses and layers. Iron oxides/hydroxides are found next to pyrite. In the upper part of the SD Formation, some cobalt peaks (up to 0.4%) can be distinguished, which are associated with the presence of carrollite (Fig. 4).

In core KW213, all members that host the orebodies are strongly altered and affected by supergene processes (Fig. 5). The Gray RAT is intensely altered and the copper grade is high (between 8 and 9.5%). Chalcocite occurs mainly as spots, but also disseminated and in veins. At the base of the DStrat, chalcocite occurs disseminated, in lenses, layers and veins. Further below, chalcocite is mainly found in silicified remains of stromatolites and in fractures. At about 500m, large nodules and bands of massive chalcocite are present, which are associated with a peak in copper (6.5%). Below this zone, copper grade diminishes in a zone with intense fracturing accompanied with large quantities of iron oxides/hydroxides. In the RSF, a strong enrichment can be observed towards the RSC. In the carbonaceous shale, which is also intensely silicified and altered, copper grade reaches over 17% due to a massive replacement of the host rock by chalcocite. The RSC is strongly silicified, altered, porous and locally fractured. Chalcocite occurs disseminated, in veins, spots and as massive replacement, which leads to a considerable copper grade (around 10%). In the Kamoto Formation, a number of minor cobalt peaks can be observed: around 495m (0.3%), between 500 and 505m (0.3%) and one around 515m (0.2%), at the base of the RSC. The peaks correspond to the occurrence of cobaltoan dolomite. No traces of carrollite were found.

The base of the SD-1a consists of a carbonaceous shale with anhydrite pseudomorphs as lenses and layers in the silty levels. Chalcocite occurs abundantly, disseminated, in the lenses and layers, as well as in veins. From 527m onwards, the dolomitic shale is pale and not as carbonaceous. Less chalcocite is present, but bornite can be observed. From about 530m, the lenses and layers disappear, but nodules occur. Chalcocopyrite can occasionally be observed in nodules and veins. At the top of the SD-1a member, a transition from a dolomitic shale to a pale dolomitic siltstone or even massive dolomite can be observed. The rock contains some lenses and layers with chalcocite and disseminated chalcocite. Copper grade is variable in this member, but often above 10%. Copper grade is much lower in the SD-2a, with some bornite and chalcocite. A distinct red alteration is spread throughout this member and the SD-2b+c. Notwithstanding the similar mineralogy, both members have a considerably lower copper grade than the SD-1a (below 2%). At the top of the SD-2b+c, only chalcocite is present, disseminated and in lenses and layers. The base of the SD-2d is carbonaceous. Although only disseminated pyrite was observed, copper content is at least the double in this zone ($\geq 4\%$). Therefore copper occurs as substitution in pyrite. In the upper part of the SD-2d, as well as in the adjacent SD-3a, bornite, chalcocite, malachite and abundant iron oxides/hydroxides can be observed. The base of the SD-3a is a zone of massive replacement by chalcocite that causes a small but distinct elevation in the copper grade (2%). Cobaltoan dolomite occurs seldom in the SD formations. Small cobalt peaks (0.1%) can be observed at the level of the carbonaceous shale and nodule horizon in the SD-2d. Higher cobalt contents occur throughout the SD-1a (0.2-0.4%), and a distinct Co peak (0.5%) coincides with the nodules horizon in the SD-1a.

The KW205 core is rather short and generally highly altered (Fig. 5). It represents the outermost part of the Kambove West megabreccia fragment. The heterogeneous breccia at the top of the core consists mostly of Gray RAT fragments. The occurrence of chalcocite in spots and veins caused a high copper grade (8%). The breccia is very rich in iron oxides/hydroxides. In the white-beige massive dolomite at the base of the CMN-I1, the ore consists of chalcocite in spots and veins. In the part immediately next to the homogeneous breccia (BH), the copper content is lower (4%). One meter below, chalcocite as well as malachite, cause again a higher copper grade (8%). In the more laminated top with less iron oxides/hydroxides, chalcocite is present. Large quantities of carrollite, spherocobaltite and cobaltoan dolomite are observed in the CMN-I1, which cause a major cobalt peak (1.9%).

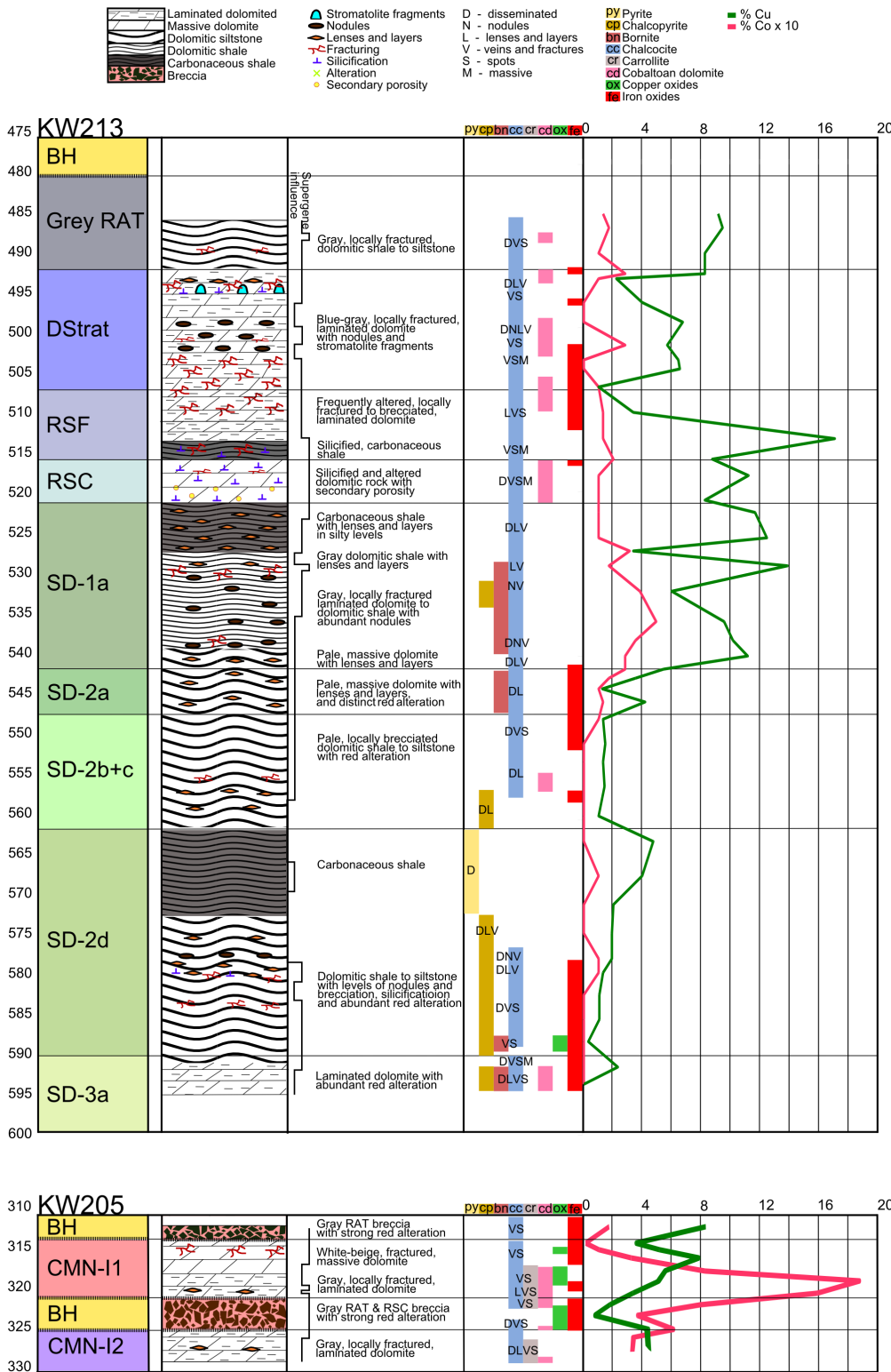


Figure 5. Stratigraphy, lithostratigraphic column, extent of the alteration, occurrence of the different ore minerals and grades of core KW213 and KW205.

The copper grade diminishes quickly towards the second zone of homogeneous breccia (1%). This second zone contains next to Gray RAT also RSC fragments. The mineralogy is quite similar, but the ore occurs in its disseminated form as well. Both the copper (4%) and cobalt (0.35%) grades increase again towards the CMN-12. In the transition zone, a minor cobalt peak (0.6%) is observed associated with the occurrence of cobaltoan dolomite. The gray, laminated dolomite of the CMN-12 contains also chalcocite, carrollite and minor cobaltoan dolomite.

5. Petrography

5.1 Methodology

Optical microscopy was used extensively for the recognition of the different mineral phases. Microscopy was performed on a

Leica DMLP, equipped for both transmitted and reflected light and with a high-resolution digital camera (DeltaPix 200). Cold cathodoluminescence petrography is used for the identification of different carbonate generations. A Technosyn Cold Cathode Luminescence Model 8200 MK II was used on a Nikon microscope. Photographs were taken with a Progres C10 camera device. Working conditions were kept constant between 10.5 to 11.0kV, 250 to 400µA and a closure time of 4.5s for photography.

5.2 Paragenesis

The paragenesis is divided in three stages according to the geological setting: the sedimentary to early diagenetic environment, diagenetic to possibly, low grade metamorphic conditions and the period of supergene alteration (Fig. 6). A further subdivision in six phases, representing an association of different gangue and

ore minerals, is used. Phase I consists dominantly of very fine-grained dolomite within the dolomitic siltstones and shales, of fine-grained pyrite and of some anhydrite nodules. Phase II and III formed during diagenesis, and are more or less similar as they consist of quartz, dolomite and sulfides. In phase II, dolomite and sulfides precipitate prior to quartz, while in phase III quartz is first. Opposed to phase II, crystals of phase III are coarse grained and sub- to euhedral. Both phases include dolomitization, veining and silicification. Only phase III shows the formation of quartz veins. In phase II, pyrite, chalcocopyrite, bornite, carrollite, digenite and chalcocite precipitated (Plate 2A). In some samples, a remarkable reverse trend can be observed: chalcocite, digenite and bornite are partly replaced by chalcocopyrite, which is thereafter replaced by pyrite (Plate 2B). During phase III, carrollite, digenite and - in particular - chalcocite precipitated (Plate 2C&D). Phase IV includes minor dolomitization and the development of few dolomite veins. The dolomite forms distinct overgrowths and veins and no replacements. Dol IV is nicely zoned, like the previous two generations. Quartz nor sulfides were observed.

Both phases V and VI formed during supergene alteration. Actually they are a continuum with an artificial border where the environment gets less reducing and copper oxides precipitated instead of sulfides. During phase V, fine-grained drowsy replacive dolomite and silica formed. Dissolution took place during the whole supergene alteration. The voids are often (partly) filled with drowsy dolomite (Dol V, and possibly VI), fine silica or large portions of chalcocite and iron oxides. During phase V, a significant part of the rocks is influenced by the remobilization of iron and copper and the precipitation of chalcocite and iron oxides in spots (Plate 2E), veins and even as a massive replacement of the host rock. Cobalt seems to be mobilized and substituted in dolomite to form cobaltoan dolomite and spherocobaltite. Phase VI is characterized by a more intense dissolution (Plate 2F) and oxidation of the previous minerals. Likewise, small spots of pseudomalachite, heterogenite and manganese oxides were observed.

5.3 Microtextures between ore minerals

Three types of microtextures between bornite and chalcocite can be distinguished (Plate 3A, B). Replacement along fractures and veinlets (type 1 from Schwartz, 1939) is by far the most commonly observed. This type can either occur during hypogene or supergene processes. Although bornite and chalcocite do not show a well-developed cleavage, replacement controlled by cleavage planes (type 2 from Schwartz, 1939) can be observed in some cases. The same interpretation can be given for the replacement along fractures and veinlets. Also replacement along boundaries (type 3 from Schwartz, 1939) with the typical rim pattern, is frequently present. This replacement has been interpreted by Schwartz (1939) as "suggestive of supergene activity, but not proof of it", because a hot fluid would be more likely to dissolve the earlier phases and consequently replace them along veins. The same three microtextures can also be observed with pyrite and

chalcocopyrite, chalcocopyrite and bornite, chalcocopyrite and chalcocite. The replacement of carrollite by chalcocite is often somewhat different (Plate 3C, D), with a multitude of chalcocite veinlets. This replacement is interpreted to be hypogene by Schwartz (1939).

5.4 Chalcocite polymorphism.

There are two polymorphs of chalcocite in the expected temperature range (Ramdohr, 1969). Low chalcocite is stable up to a temperature of 103°C and can have multiple ways of formation: 1) from hypogene solutions below 103°C, 2) paramorphically from high chalcocite crystals formed above 103°C, and 3) from supergene solutions (Ramdohr, 1969). High chalcocite is formed from hypogene solutions between 103°C to 435°C (Posfai & Buseck, 1994). Two microtextures in chalcocite can be linked to these polymorphs (Ramdohr, 1969). A lamellar texture consists of lenticular bodies of up to 200µm in length and about 1 to 10µm wide, which vary slightly in color from bluish purple to pale blue anisotropy (Plate 3E, F). These inversion lamellae and the segmental pattern parallel to the (0001) mineral planes indicate the former presence of hexagonal chalcocite, which is interpreted to be high chalcocite. Low chalcocite can have an orthorhombic texture, which consists of polygonal crystals that are 10 to 50µm in diameter and have a similar anisotropy. The crystals in which both the textures were observed, are very large (up to 1 cm) and occur in altered and chalcocite-rich, massive dolomites (Dol III, IV, V and the cobaltoan VI) of the Lower CMN. The presence of the lamellar texture proves that at least part of the chalcocite crystallized above 103°C and is thus of hypogene origin. But whether all the orthorhombic crystals are truly indicative for low chalcocite and, therefore, formed below 103°C remains uncertain.

6. Discussion

6.1 Ore grades

Historically, a cut-off grade of 3 to 4% copper has been used in the case of the Kambove West deposit for the delineation of the orebody (Cailteux, 1983; Gécamines, UMHK). In most samples, the mineralogy is quite homogeneous. The ore mineral assemblage is mostly similar in the veins, disseminated and in spots. Sometimes one can observe that the veins enriched the surrounding host rock.

An enrichment in copper in the RSC can be seen in borehole KW201bis. This trend is also reflected in the mineralogy. A transition from pyrite to chalcocopyrite, bornite and finally chalcocite can be observed from the SD3 (pyrite at 540m) to the RSC (chalcocite at several intervals between 477 - 404m). Veins, which typically formed during the hypogene mineralization, were observed in all members of the Mines Subgroup. In the orebodies, veins are abundant and generally contain a lot of ore minerals and result in an enrichment of the surrounding rocks. In barren or poor zones,

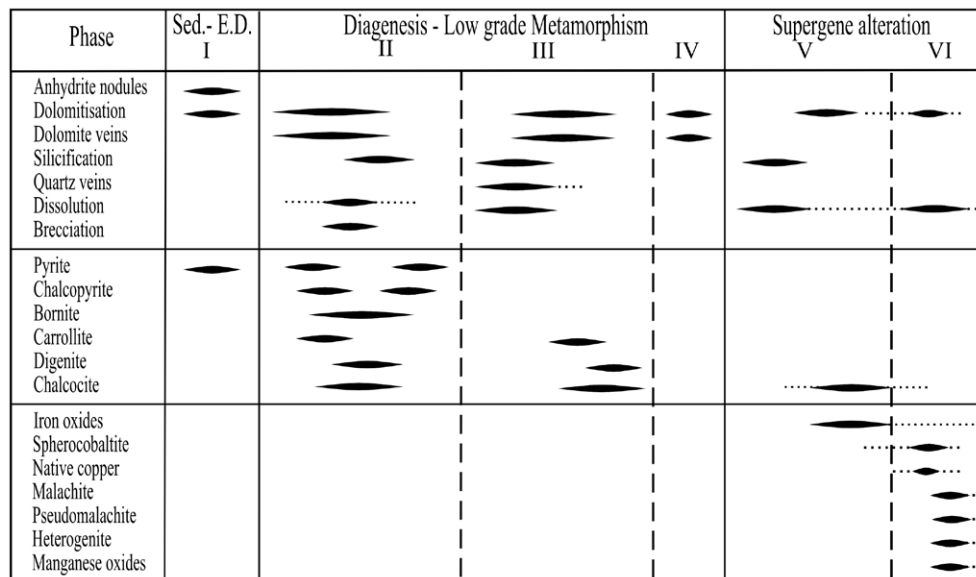


Figure 6. Paragenesis of the Kambove-West deposit. Time flows from left to right. Full vertical lines divide the three major phases, while dashed lines subdivide minor phases. Sed.-E.D.; Syn-sedimentary to very early diagenetic.

significantly fewer veins were observed. The veins are thinner and are also poorly mineralized. These observations are in accordance with the model of Fay & Barton (2012), in which the RSC acts as fluid pathway.

In and adjacent to brecciated zones, a distinct more intense supergene enrichment and an increase in copper content can be seen (e.g. KW205). These brecciated zones form permeable pathways and allow the infiltration of metal-bearing, supergene fluids. Supergene enrichment in chalcocite occurred when these metal-bearing fluids reached the sulfide-bearing strata.

Another characteristic feature associated with mineralization are stromatolite fragments. These silicified fragments are often well-mineralized by chalcocite and carrollite or cobaltoan dolomite. Carrollite likely formed in zones with a very high sulfur activity (Craig et al., 1979; Muchez et al., 2008). In the stromatolite fragments, sulfur presumably originated from sulfate-reducing microorganisms, which were main components of Precambrian stromatolite communities (Dillon, 2011). A similar association was also found between carrollite and anhydrite pseudomorphs (e.g.: KW201bis: 462m). However, this association is not always as obvious as described in Muchez et al. (2008) and El Desouky et al. (2010).

Remarkable enrichments in copper were also found in carbonaceous zones. In and adjacent to the RSC, carbonaceous dolomites or dolomitic shales are present (e.g.: KW201bis: 445m and 457m). Spots and massive replacements by chalcocite are frequently observed, as well as the occurrence of chalcocite in nodules, lenses, layers and veins, and to a lesser extent also disseminated. The presence of organic matter caused a reducing environment. The carbonaceous zones are also often highly altered. Especially the chalcocite spots and massive replacements seem to be closely associated with supergene processes. These enrichments resulted in the major copper peaks and thus the irregular distribution in the RSC.

The base of the SD-1a and SD-2d have a very similar lithology, but their mineralogy and average grade differ greatly. The grades in SD-1a are about three times higher than in SD-2d. Both hypogene and supergene processes account for the large differences in grade. However, as especially the chalcocite spots and massive replacements are responsible for the high grades, likely supergene processes are more important. Next to features that correlate with an increase in copper and cobalt grades, certain factors can be linked to a decrease in ore grade. In zones with a very large permeability, presumably caused by brecciation or dissolution associated with silicification, chalcocite is frequently partly dissolved. In intensely iron oxide/hydroxide-stained zones, grades are often very low (e.g.: KW201bis: 450-455m). A distinct oxidation is usually affiliated with fracturing or brecciation. The iron oxide/hydroxides precipitated by a supergene fluid in an oxidizing environment. This fluid likely also dissolved copper- and cobalt-minerals, as demonstrated by Ague & Brimhall (1989). This type of “red alteration” is in contrast to the “gray alteration”, which occurred in a reducing environment and resulted in enrichment. The iron oxides/hydroxides are mainly goethite. This is not surprising since goethite is the most stable under low temperature conditions in both alkaline and acidic environments (Smith & Kidd, 1949).

6.2 Paragenesis

The multiphase origin proposed by Cailteux et al. (2005b), Muchez et al. (2008), El Desouky et al. (2010), Haest & Muchez (2011) and Fay & Barton (2012) for the Katanga Copperbelt is also applicable for the Kambove West ore deposit. The paragenetic sequence reconstructed for the Kambove West deposit is discussed below within the metallogenic model proposed for the Katanga Copperbelt by these different authors. In contrast with these studies, special attention is given at the supergene processes.

The host rocks of the Mines Subgroup were deposited in a sabkha to lagoonal environment (e.g. Cailteux, 1983). The shaly units of the SD formations were deposited in lagoons, whilst stromatolites and algal reefs grew in intratidal zones. Lithofacies variations proved to be of uttermost importance for the ore distribution. During early diagenesis, the rocks were dolomitized and fine-grained pyrite as well as anhydrite nodules, lenses and layers

were formed. Anhydrite pseudomorphs occur as nodules, lenses and layers.

Ore formation occurred during diagenesis, but before final compaction and lithification. Conform the models of Fay & Barton (2012) and Muchez & Corbella (2012), it is proposed that a hydrothermal fluid transported metals through the RSC, into the adjacent strata (Fig. 7A, B). A sequence of dolomite, sulfides and quartz precipitated. According to the reaction mechanisms reported by Muchez et al. (2008), bicarbonate and hydrogen sulfide were released when the sulfates of the anhydrite were reduced by BSR. The bicarbonate is used in the precipitation of dolomite. The reduced sulfur reacted with the metals to form sulfides. These reactions explain the observed association of dolomite (Dol II) with sulfides in the lenses and layers, and in the outer part of the nodules. The latter two reactions also caused the release of hydrogen-ions, which lowered the pH significantly. At a low pH, the solubility of silica is limited and authigenic quartz (Qtz II) precipitated in the core of the nodules and also replaced the dolomite. The mineralization was not restricted to these nodules, layers and lenses. The original fine-grained Dol I was intensely replaced by Dol II and Qtz II. The fluids locally fractured the host rock and formed veins. Sulfur was available in the host rock and allowed sulfides to form in these veins, but also disseminated in the host rock. The replacement of early diagenetic pyrites has been observed, which implies that they formed at least part of the sulfur source (Dewaele et al., 2006). A mineral sequence of pyrite, chalcopyrite, bornite, carrollite, chalcocite, digenite, chalcopyrite and pyrite was observed in the present study. The first part is a continuous copper enrichment, as is expected for a copper carrying fluid (Muchez & Corbella, 2012). The occurrence of late chalcopyrite and pyrite is difficult to explain as there are no direct indications of what may have caused this trend and since it does not correspond with the common evolution trend of Cu-Co-rich fluids. However, similar successions were observed in Cailteux (1983, 1994) and future reactive transport modeling could provide an explanation for this reverse trend. A possibility to consider is that later fluids were poor in copper and cobalt and carried iron in solution.

The second main mineralization phase took place during late diagenesis or low-grade metamorphism (Fig. 7C). Silicification, dissolution and quartz veins preceded dolomitization and dolomite veins and the associated sulfides. The antecedent dissolution allowed the Dol III crystals to grow freely. This fluid further enriched the host rock in copper and cobalt by precipitation of carrollite, chalcocite and minor digenite. The previous veins, lenses,

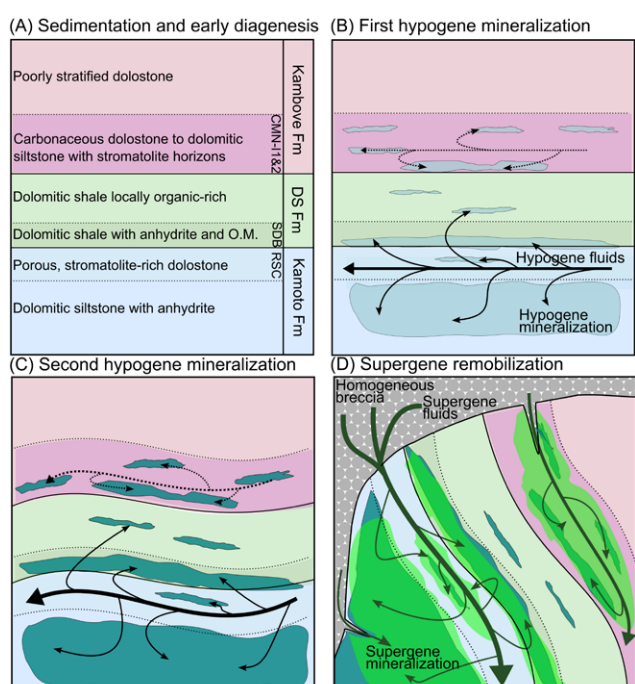


Figure 7. Mineralization model with two hypogene mineralizations and one supergene remobilization (partly after Fay & Barton, 2012).

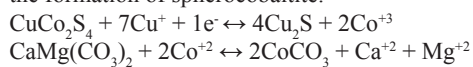
layers and nodules are often recrystallized, but also new veins were formed. When the host rock was dolomitized by Dol III, also disseminated sulfides were formed by the passing fluids. A fourth, brownish, generation of dolomite (Dol IV) was confirmed by the use of cold cathodoluminescence microscopy. This phase is found mainly in veins crosscutting the previous vein generations. Notwithstanding this generation is thought to be of hypogene origin, no mineralization is associated with the dolomite. The exact timing of this dolomite generation remains unclear.

During weathering, copper and cobalt dissolved in the leached zone by meteoric fluids (Fig. 7D). These metal-enriched fluids migrated further downwards and the dissolved metals precipitated again in the supergene blanket (cementation zone). Above the redox barrier, metals precipitate as oxides (mainly malachite), whilst under the redox barrier, mineralization occurs as sulfides (mainly chalcocite). Minor authigenic quartz is accompanied with a dissolution phase. When the supergene waters reached equilibrium with the host rock, a dolomite (Dol V) precipitated together with chalcocite.

Many indications of a strong enrichment in chalcocite were found. Macroscopically, a close association of spots and of massive replacement by chalcocite with altered zones was observed. These altered zones occur typically in or near the porous RSC or a brecciated zone, which could have acted as fluid conduits. As the southern flank of the Kambove West syncline stands vertical, the RSC is optimally orientated for supergene fluids to flow to deep zones. Microscopic indications of the copper and cobalt remobilization were also found: replacement of hypogene ore minerals along boundaries (especially the rim pattern) by chalcocite, irregular chalcocite spots and veinlets in altered zones with alteration dolomites (Dol V and VI) and the orthorhombic microtexture in chalcocite, which is mostly formed by supergene remobilization. Spots of native copper and malachite also indicate the presence of supergene processes.

The association of chalcocite with iron oxides/hydroxides is also indicative for a formation during supergene enrichment. Such an association is in accordance with the fact that during precipitation of secondary sulfides, H^+ is released which caused the pH to decrease to about 3.5. A mixture of goethite and hematite is preferentially formed by aging of ferrihydrate at this pH (Ague & Brimhall, 1989; Alpers & Brimhall, 1989). In poorly mineralized zones, less H^+ was released, consequently the pH was more neutral and more hematite was formed. Goethite turns to hematite by a dehydration reaction. In order for this reaction to continue, oxygen must be available (Turner, 1974). The iron originated from iron hydroxides (Cailteux, 1983), which is in its turn a product of the oxidation of pyrite and chalcopyrite. The stability field of goethite is in addition to Eh and pH also very dependent on the activity of aluminum (also trivalent), grain size, water activity, kinetic effects, presence of organic material and the concentrations of other dissolved ions (Berner, 1969; Ague & Brimhall, 1989; Alpers & Brimhall, 1989). It is also probable that hematite and goethite were formed from a metastable phases like ferrihydrite (Schwertmann & Murad, 1983; Alpers & Brimhall, 1989). Relatively high amounts of goethite were detected in samples with a low chalcocite content, which is in accordance with the previous statements.

The presence of spherocobaltite and cobaltoan dolomite (Dol VI) is also thought to be a consequence of supergene processes. The cobalt was presumably released when carrollite dissolved to the expense of chalcocite formation. The released Co^{+3} is, however, not stable (Craig et al., 1979) and will be reduced to Co^{+2} , which substitutes in dolomite. By partial substitution, cobaltoan dolomite can be formed, while complete substitution results in the formation of spherocobaltite.



In certain porphyry copper systems, a fivefold rise of the grades has been reported (Ague & Brimhall, 1989). Such an increase is certainly realistic in certain zones of the Kambove West deposit.

The hypogene and supergene processes described above were found to be similar for the Katanga Copperbelt (Cailteux et al., 2005b; Dewaele et al., 2006; Fay & Barton, 2012). In general, it can be stated that the mineralization in the Katanga Copperbelt

is relatively uniform, with two major hypogene stages and one supergene remobilization stage. The latter can be subdivided in two phases (Fig. 6).

7. Conclusion

Key factors that play a significant role in the development of high-grade ore at Kambove West are the extent of alteration, the presence of organic matter, anhydrite pseudomorphs, early generations of sulfides and, to a lesser extent, stromatolite fragments. Beige-gray (altered) or black (carbonaceous) zones typically contain much higher grades than red zones (leached and oxidized). The stratigraphic position of mineralized zones adjacent to the RSC and brecciated zones are the most relevant factor in the formation of a high-grade mineralization, since the RSC and brecciated zones acted as the major fluid conduits.

The paragenesis consists of six major phases. During a first sedimentary to early diagenetic stage a sabkha dolomite containing fine-grained pyrite and anhydrite nodules, lenses and layers was deposited. The second and third phases took place during diagenesis and low-grade metamorphism. Both manifested themselves through silicification, dissolution, dolomitization, veining and the precipitation of Cu-Co sulfides. A fourth phase, of lesser importance, consists merely of one generation of dolomite. The fifth and sixth phases occurred during the supergene stage. The fifth phase consists of silicification and dissolution, followed by the precipitation of dolomite, iron oxides/hydroxides and large amounts of chalcocite. During the sixth phase, a cobaltoan dolomite replaced earlier dolomites. Iron, copper, cobalt and manganese oxides precipitated, accompanied by a final dissolution phase. The supergene chalcocite, which precipitated during the fifth phase, can be differentiated from the hypogene minerals by multiple features. A first feature is the replacement of hypogene ore minerals along boundaries by chalcocite (rim pattern). Secondly, irregular spots, veinlets and replacement of host rock by massive chalcocite associated with altered zones can be observed both macro- and microscopically. Thirdly, chalcocite with an orthorhombic microtexture mainly formed through supergene remobilization. Finally, the association of chalcocite with spots of iron oxides/hydroxides (especially goethite), native copper and copper oxides likewise reveals a supergene influence. However, none of these four features provide conclusive evidence of a supergene origin, but the presence of one or more of these features is nevertheless considered highly suggestive. Notwithstanding an exact ratio is not available at the moment, it can be concluded that supergene remobilization is a very important process since in all high grade zones signs of supergene alteration are found.

8. Acknowledgments

We would like to thank the Société de Gécamines, and especially ir. Gilbert Kalamba Banika, director of the Mines and Quarries, for the permission to study the cores of the Kambove West deposit. We greatly appreciate the help of Mr. Bombile and Mr. Petrov, both of the Société de Gécamines, during the selection and sampling of the cores at Likasi. We are grateful to dr. Fred Kamona and dr. Johan Yans for the constructive reviews and to dr. Jean-Clair Duchesne for careful editorial handling. We also thank drs Jorik Van Wilderode, Rieko Adriaens and Koen Torremans for stimulating discussions. Herman Nijs kindly prepared the thin and polished sections. This research is financially supported by research grant G.04174.08 from the FWO-Vlaanderen (Belgium).

9. References

- Ague, J. & Brimhall, G., 1989. Geochemical modeling of steady state fluid flow and chemical reaction during supergene enrichment of porphyry copper deposits. *Economic Geology* 84, 506-528.
- Alpers, C. & Brimhall, G., 1989. Paleohydrologic evolution and geochemical dynamics of cumulative supergene metal enrichment at La Escondida, Atacama Desert, northern Chile. *Economic Geology* 84, 229-255.
- Armstrong, R., Master, S. & Robb, L., 2005. Geochronology of the Nchanga Granite, and constraints on the maximum age of the Katanga Supergroup, Zambian Copperbelt. *Journal of African Earth Sciences* 42, 32-40.

- Batumike, M., Cailteux, J. & Kampunzu, A., 2007. Lithostratigraphy, basin development, base metal deposits, and regional correlations of the Neoproterozoic Nguba and Kundelungu rock successions, central African Copperbelt. *Gondwana Research* 11, 432-447.
- Berner, R., 1969. Goethite stability and the origin of red beds. *Geochimica et Cosmochimica Acta* 33, 267-273.
- Brems, D., Muchez, P., Sikazwe, O. & Mukumba, W., 2009. Metallogenesis of the Nkana copper-cobalt South Orebody, Zambia. *Journal of African Earth Sciences* 55, 185-196.
- Broughton, D.W. & Rogers, T., 2010. Discovery of the Kamoia copper deposit, Central African Copperbelt, D.R.C.. *Society of Economic Geologists, Special Publication* 15, 287-297.
- Cahen, L., François, A. & Ledent, D., 1971. Sur l'âge des uraninites de Kambove Ouest et de Kamoto Principal et révision des connaissances relatives aux minéralisations uranifères du Katanga et du Copperbelt de Zambia. *Annales de la Société Géologique de Belgique* 94, 185-198.
- Cailteux, J., 1977. Particularités stratigraphiques et pétrographiques du faisceau inférieur du Groupe des Mines au centre de l'Arc Cuprifère Shabien. *Annales de la Société Géologique de Belgique* 100, 55-71.
- Cailteux, J., 1979. L'origine du talc dans le C.M.N. (ou R.2.3) de Kambove (Shaba, Zaire). *Annales de la Société Géologique de Belgique* 102, 213-221.
- Cailteux, J., 1983. Le Roan Shabien dans le Région de Kambove (Shaba, Zaire). *Etude sédimentologique et métallogénique.*, Université de Liège.
- Cailteux, J., 1986. Diagenetic sulphide mineralization within the stratiform copper-cobalt deposit of West Kambove (Shaba-Zaire); sequence of mineralization in sediment-hosted copper deposits (Part 2). *Special Publication of the Society for Geology Applied to Mineral Deposits* 4, 398-411.
- Cailteux, J., 1994. Lithostratigraphy of the Neoproterozoic Shaba-type (Zaire) Roan Supergroup and metallogenesis of associated stratiform mineralization. *Journal of African Earth Sciences* 19, 279-301.
- Cailteux, J., 1997. Minéralisations à U-Pb-Se-Mo-Ni dans le gisement stratiforme cupro-cobaltifère de Kambove-Ouest (Shaba, Rep. Zaire). In Charlet J-M (ed.) *International Cornet Symposium 'Stratabound Copper Deposits and Associated Mineralizations'*. Faculté Polytechnique de Mons and Royal Academy of Overseas Sciences, Liège, 245-286.
- Cailteux, J. & Kampunzu, H. A. B. 1994. The Katangan tectonic breccias in the Shaba Province (Zaire) and their genetic significance. *Annalen Koninklijk Museum voor Midden-Afrika. Geologische Wetenschappen* 101, 63-76.
- Cailteux, J., Kampunzu, A. & Batumike, M., 2005a. Lithostratigraphic position and petrographic characteristics of R.A.T. (Roches Argilo-Talqueuses) Subgroup, Neoproterozoic Katangan Belt (Congo). *Journal of African Earth Sciences* 42, 82-94.
- Cailteux, J., Kampunzu, A., Lerouge, C., Kaputo, A. & Milesi, J., 2005b. Genesis of sediment-hosted stratiform copper-cobalt deposits, central African Copperbelt. *Journal of African Earth Sciences* 42, 134-158.
- Cosi, M., De Bonis, A., Gosso, G., Hunziker, J., Martinotti, G., Moratto, S., Robert, J. & Ruhlman, F., 1992. Late Proterozoic thrust tectonics, high-pressure metamorphism and uranium mineralization in the Domes Area, Lufilian Arc, Northwestern Zambia. *Precambrian Research* 58, 215-240.
- Craig, J. R., Vaughan, D. J. & Higgins, J. B., 1979. Phase relations in the Cu-Co-S system and mineral associations of the carrollite (CuCo₂S₄)-linnaeite (Co₃S₄) series. *Economic Geology* 74, 657-671.
- Decree, S., Delouie, E., Ruffet, G., Dewaele, S., Mees, F., Marignac, C., Yans, J. & De Putter, T., 2010. Geodynamic and climate controls in the formation of Mio-Pliocene world-class oxidized cobalt and manganese ores in the Katanga Province, D. R. Congo. *Mineralium Deposita* 45, 621-629.
- de Magnee, I. & François, A. 1988. The origin of the Kipushi (Cu,Zn,Pb) deposit in direct relation with a Proterozoic salt diapir, Copperbelt of Central Africa, Shaba, Republic of Zaire. *Special Publication of the Society for Geology Applied to Mineral Deposits* 5, 74-93.
- De Putter, T., Mees, F., Decrée, S. & Dewaele, S., 2010. Malachite, an indicator of major Pliocene Cu remobilization in a karstic environment (Katanga, Democratic Republic of Congo). *Ore Geology Reviews*, 38, 90-100.
- Dewaele, S., Muchez, P., Vets, J., Fernandez-Alonzo, M. & Tack, L., 2006. Multiphase origin of the Cu-Co ore deposits in the western part of the Lufilian fold-and-thrust belt, Katanga (Democratic Republic of Congo). *Journal of African Earth Sciences* 46, 455-469.
- Dillon, J. 2011. The role of sulfate reduction in stromatolites and microbial mats: ancient and modern perspectives. In Tewari, V. & Seckbach, J. (Ed.), *Stromatolites: Interaction of Microbes with Sediments*, Springer Netherlands.
- El Desouky, H., Muchez, P., Dewaele, S., Boutwood, A. & Tyler, R., 2008. Postorogenic origin of the stratiform Cu mineralization at Lufukwe, Lufilian Foreland, Democratic Republic of Congo. *Economic Geology* 103, 555-582.
- El Desouky, H., Muchez, P. & Cailteux, J., 2009. Two Cu-Co sulfide phases and contrasting fluid systems in the Katanga Copperbelt, Democratic Republic of Congo. *Ore Geology Reviews* 36, 315-332.
- El Desouky, H., Muchez, P., Boyce, A., Schneider, J., Cailteux, J., Dewaele, S. & von Quadt, A., 2010. Genesis of sediment-hosted stratiform copper-cobalt mineralization at Luiswishi and Kamoto, Katanga Copperbelt (Democratic Republic of Congo). *Mineralium Deposita* 45, 735-763.
- Fay, I. & Barton, M., 2012. Alteration and ore distribution in the Proterozoic Mines Series, Tenke-Fungurume Cu-Co district, Democratic Republic of Congo. *Mineralium Deposita* 47, 1-19.
- François, A., 1974. Stratigraphie, tectonique et minéralisations dans l'arc cuprifère du Shaba (République du Zaïre). In *Gisements stratiformes et provinces cuprifères*. Société Géologique de Belgique, 79-101.
- François, A., 1987. Synthèse géologique sur l'arc cuprifère du Shaba (Rep. du Zaïre). *Bulletin de la Société Belge de Géologie, Hors Serie*, 15-65.
- François, A., 2006. La partie centrale de l'Arc cuprifère du Katanga: étude géologique. *Musée Royal de l'Afrique Centrale, Tervuren*.
- Haest, M. & Muchez, P., 2011. Stratiform and vein-type deposits in the Pan-African orogen in central and southern Africa: evidence for multiphase mineralisation. *Geologica Belgica* 14, 23-44.
- Hitzman, M., Kirkham, R., Broughton, D., Thorson, J. & Selley, D., 2005. The sediment-hosted stratiform copper ore system. *Economic Geology 100th Anniversary Volume*, 609-642.
- International Bank for Reconstruction and Development, 1974. Report No 576a-CK: Appraisal of Gecamines Project.
- Jackson, M., Warin, O., Woad, G. & Hudec, M., 2003. Neoproterozoic allochthonous salt tectonics during the Lufilian orogeny in the Katangan Copperbelt, Central Africa. *Geological Society of America Bulletin* 115, 314-330.
- Johnson, S., De Waele, B., Evans, D., Banda, W., Tembo, F., Milton, J. & Tani, K., 2007. Geochronology of the Zambezi supracrustal sequence, southern Zambia; a record of Neoproterozoic divergent processes along the southern margin of the Congo Craton. *Journal of Geology* 115, 355-374.
- Kampunzu, A. & Cailteux, J., 1999. Tectonic Evolution of the Lufilian Arc (Central Africa Copper Belt) during Neoproterozoic Pan African Orogenesis. *Gondwana Research* 2, 401-421.
- Kampunzu, A., Tembo, F., Matheis, G., Kapenda, D. & Huntsman-Mapila, P., 2000. Geochemistry and Tectonic Setting of Mafic Igneous Units in the Neoproterozoic Katangan Basin, Central Africa: Implications for Rodinia break-up., *Gondwana Research* 3, 125-153.
- Misra, K., 2000. *Understanding mineral deposits*. Kluwer Academic, Dordrecht.
- Muchez, P. & Corbella, M., 2012. Factors controlling the precipitation of copper and cobalt minerals in sediment-hosted ore deposits: Advances and restrictions. *Journal of Geochemical Exploration* 118, 38-46.
- Muchez, P., Vanderhaeghen, P., El Desouky, H., Schneider, J., Boyce, A., Dewaele, S. & Cailteux, J., 2008. Anhydrite pseudomorphs and the origin of stratiform Cu-Co ores in the Katangan Copperbelt (Democratic Republic of Congo). *Mineralium Deposita* 43, 575-589.
- Muchez, P., Brems, D., Clara E. and De Cleyn, A., Lammens, L., Boyce, A., De Muynck, D., Mukumba, W. & Sikazwe, O., 2010. Evolution of Cu-Co mineralizing fluids at Nkana Mine, Central African Copperbelt, Zambia. *Journal of African Earth Sciences* 58, 457-474.
- Porada, H. & Berhorst, V., 2000. Towards a new understanding of the Neoproterozoic-early Palaeozoic Lufilian and northern Zambezi belts in Zambia and the Democratic Republic of Congo. *Journal of African Earth Sciences* 30, 727-771.
- Posfai, M. & Buseck, P., 1994. Djurleite, digenite, and chalcocite; intergrowths and transformations. *American Mineralogist*, 79, 308-315.
- Prasad, M., 1989. Production of copper and cobalt at Gecamines, Zaire. *Minerals Engineering* 2, 521-541.
- Ramdohr, P., 1969. *The ore minerals and their intergrowths*. Pergamon Press, Oxford.
- Robb, L., 2005. *Ore-forming processes*. Blackwell Science Ltd, Oxford.
- Schwartz, G. M., 1939. Significance of bornite-chalcocite microtextures. *Economic Geology* 34, 399-418.
- Schwertmann, U. & Murad, E., 1983. Effect of pH on the formation of goethite and hematite from ferrihydrite. *Clays and Clay Minerals* 31, 277-284.

- Selley, D., Broughton, D., Scott, R., Hitzman, M., Bull, S., Large, R., McGoldrick, P., Croaker, M., Pollington, N. & Barra, F. 2005. A new look at the geology of the Zambian Copperbelt. *Economic Geology* 100th Anniversary volume, 965-1000.
- Smith, F. & Kidd, D., 1949. Hematite-goethite relations in neutral and alkaline solutions under pressure. *American Mineralogist* 34, 403-412.
- Sweeney, M.A. & Binda, P.L., 1994. Some constraints on the formation of the Zambian Copperbelt deposits. *Journal of African Earth Sciences* 19, 303-316.
- Sweeney, M.A., Binda, P.L. & Vaughan, D.J., 1991. Genesis of the ores of the Zambian Copperbelt. *Ore Geology Reviews* 6, 51-76.
- Turner, P., 1974. Origin of red beds in the Ringerike Group (Silurian) of Norway. *Sedimentary Geology* 12, 215-235.
- Webb, M. & Rowston, P., 1995. The Geophysics of the Ernest Henry Cu-Au Deposit (NW) Qld. *Exploration Geophysics* 26, 51-59.

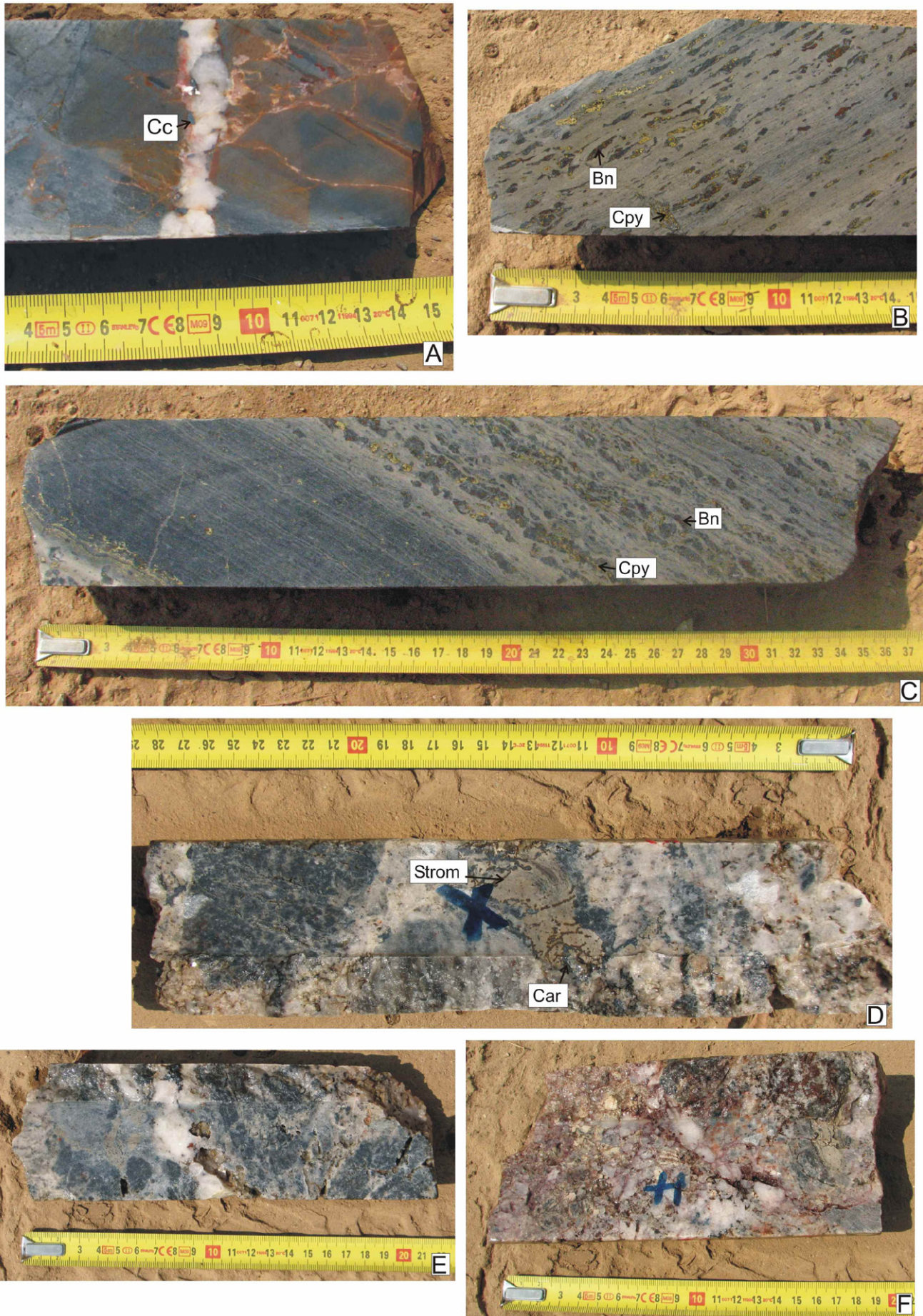


Plate 1. A. Chalcocite (Cc) in coarse crystalline vein. B & C Chalcopyrite (Cpy) and bornite (Bn) in nodules and lenses along the bedding planes. D. Close association of stromatolite fragments and carrollite. E. RSC characterized by silicification and dissolution. F. RSC showing silicification, dissolution and the occurrence of iron oxides/hydroxides.

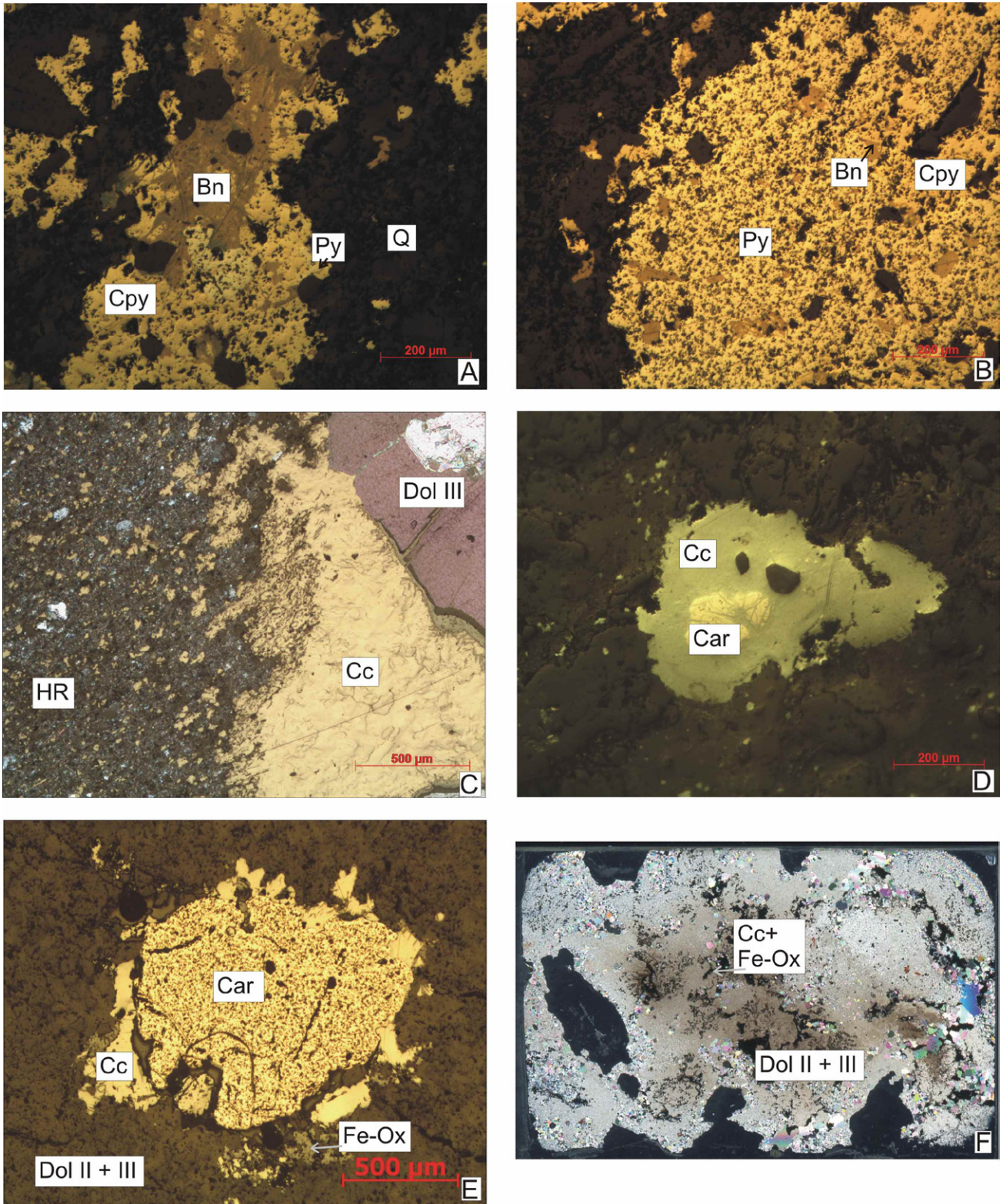


Plate 2. A & B. Chalcopyrite (Cpy), with relicts of pyrite (Py), is partly replaced by bornite (Bn) (SD-1a). C. Chalcocite (Cc) from a Dol III vein in DS (HR: host rock). D. Spot of carrollite (Car) that is partly replaced by chalcocite (Cc) in Gray RAT. E. Rim of chalcocite (Cc) and iron oxides/hydroxides (Fe-Ox) around carrollite (Car) in the CMN-11. F. Irregular dissolution and precipitation of dolomite (Dol II + III), chalcocite (Cc) and iron oxides/hydroxides (Fe-Ox) in the RSC.

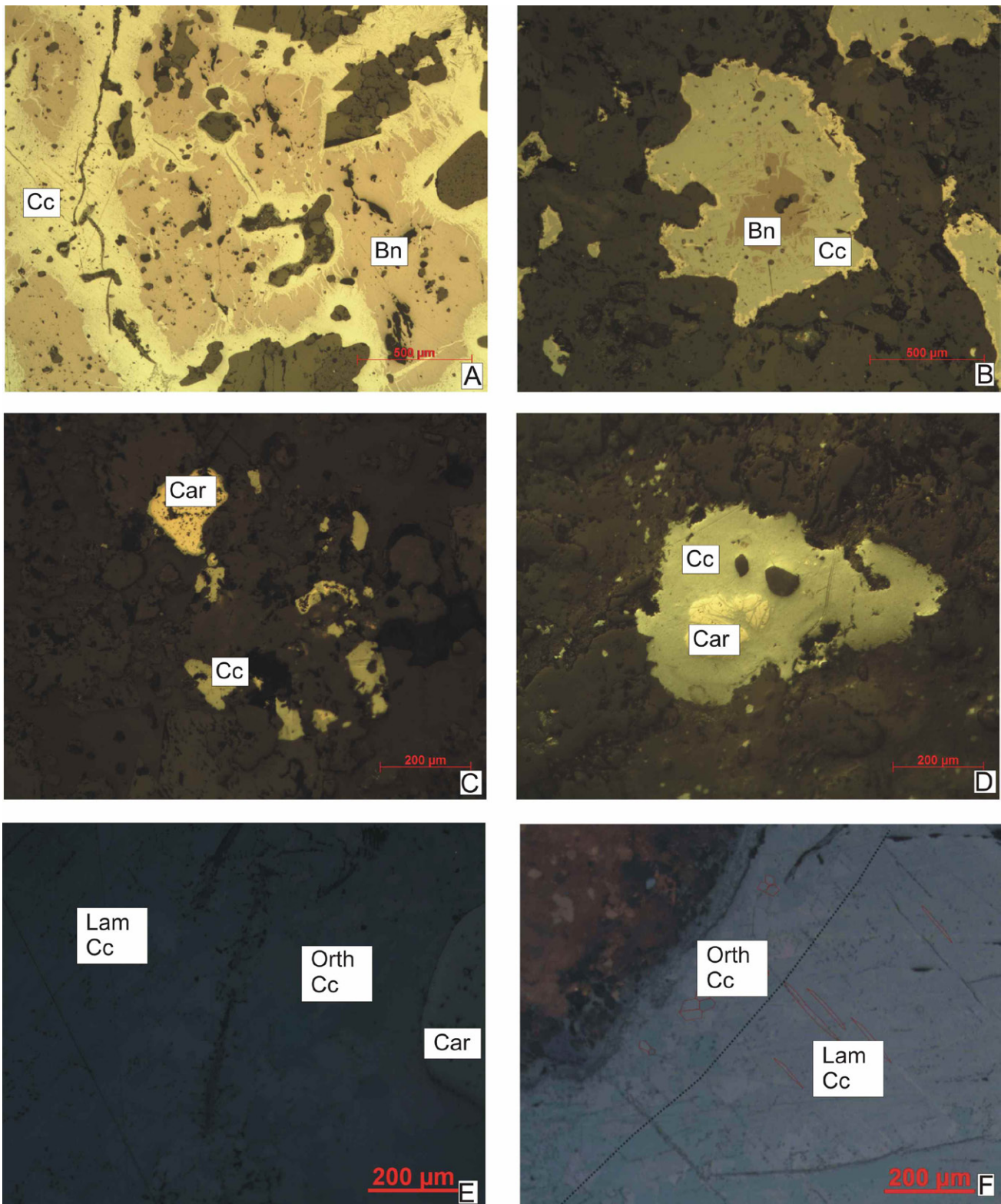


Plate 3. A, B and C. Microtextures between the different sulfides and especially bornite (Bn), chalcocite (Cc) and carrollite (Car) D. Replacement of carrollite (Car) by chalcocite (Cc). E. Lamellae (Lam Cc) indicating the former presence of hexagonal chalcocite in orthorhombic chalcocite (Orth Cc) next to carrollite (Car). F. Lamellae (Lam Cc) in orthorhombic (Orth Cc) chalcocite.